Structures of Rydberg transitions in the absorption spectra of methyl-substituted derivatives of bis(η^6-benzene)chromium

S. Yu. Ketkov,[a] G. A. Domrachev,[a] C. P. Mehnert,[b] and J. C. Green[b]*

[a]*G. A. Razuvaev Institute of Organometallic Chemistry, Russian Academy of Sciences, 49 ul. Tropinina, 603600 Nizhnii Novgorod, Russian Federation. Fax: +7 (831 2) 66 1497*

[b]*Inorganic Chemistry Laboratory, University of Oxford, Oxford OX1 3QR, Great Britain. Fax: (01865) 27 2690*

The effect of methylation of ligands in bis(η^6-benzene)chromium (**1**) on the structure of Rydberg transitions in absorption spectra has been studied. A detailed analysis and interpretation of all Rydberg elements of the vapor-phase spectra of bis(η^6-toluene)chromium (**2**), bis(η^6-*o*-xylene)chromium (**3**), bis(η^6-*m*-xylene)chromium (**4**), and bis(η^6-mesitylene)chromium (**5**) was carried out. The vapor-phase electronic absorption spectrum of bis(η^6-*p*-xylene)chromium (**6**) was measured, and the assignment of the Rydberg bands was made for the first time. The first ionization potentials of complexes **2**—**5** were refined. The energy of detachment of the $3d_{z^2}$ electron and the parameters of the Rydberg excitations for molecule **6** were determined. The vibronic components of the $3d_{z^2} \rightarrow R4p_{x,y}$ transition in the spectra of complexes **2** and **6** were assigned. The differences in the Rydberg structure of the spectra of compounds **2**—**6** were analyzed in terms of the selection rules for optical transitions in the corresponding symmetry groups. The vapor-phase spectra correspond to conformers with the symmetry groups C_{2v} and C_2 for complexes **2**—**4**, with the symmetry groups D_{3h} and D_3 for compound **5**, and with the symmetry group D_{2d} for complex **6**.

Key words: bisarenechromium complexes, methyl-substituted derivatives of bis(η^6-benzene)chromium, molecular symmetry; electronic absorption spectra, Rydberg transitions.

Sandwich complexes of transition metals are of interest as objects for studying by electronic absorption spectroscopy because they represent the only class of organometallic compounds whose vapor-phase absorption spectra have clearly defined Rydberg bands. Rydberg transitions can form series that converge to the ionization limit. The frequencies of the members of the series are described by the well-known Rydberg formula:[1]

$$\nu_n = I - R/(n - \delta)^2 = I - R/(n^*)^2 = I - T,$$

where I is the energy of detachment of an electron from the orbital involved in the Rydberg transition (ionization limit); R is the Rydberg constant (109737 cm^{-1}); n is the principal quantum number; δ is the quantum defect; n^* is the effective principal quantum number; and T is the term value (the energy of binding of the Rydberg electron with the cationic core).

The Rydberg series can be assigned to particular transitions based on the quantum defects. The assignment of low-lying Rydberg excitations was usually made with the use of term values that are similar to those of the corresponding excitations in the molecules with analogous structures.[1] The frequencies of Rydberg bands are related to ionization potentials (*IP*), and their structures characterize the molecular and electronic structures of compounds.[1] Therefore, studies of Rydberg excitations in molecules of sandwich complexes provide valuable data on the effect of various factors on the ionization characteristics and mutual arrangement of electronic levels.

Previously,[2—9] it has been demonstrated that in the vapor-phase spectra of a number of alkyl-substituted derivatives of $(\eta^6\text{-}C_6H_6)_2Cr$ (**1**), most of the bands correspond to Rydberg transitions from the $3d_{z^2}$ orbital of the Cr atom. Introduction of methyl groups (from one to three) into each benzene ring of compound **1** results in a change in the vapor-phase spectrum, while the spectrum of the complex in the condensed phase remains virtually unchanged. Recently,[10] Rydberg transitions in the spectrum of $(\eta^6\text{-}C_6H_6)_2Cr$ have been studied in detail. In this work, we carried out a detailed study of the spectra of the complexes $(\eta^6\text{-PhMe})_2Cr$ (**2**), $(\eta^6\text{-}1,2\text{-}Me_2C_6H_4)_2Cr$ (**3**), $(\eta^6\text{-}1,3\text{-}Me_2C_6H_4)_2Cr$ (**4**), and $(\eta^6\text{-}1,3,5\text{-}Me_3C_6H_3)_2Cr$ (**5**), which have been briefly discussed in previous works.[2—9] To obtain a more detailed view of the effect of methyl substituents in benzene rings on the energies of the excited states of $(\eta^6\text{-arene})_2Cr$, we studied the vapor-phase absorption spectrum of the complex $(\eta^6\text{-}1,4\text{-}Me_2C_6H_4)_2Cr$ (**6**) for the first time.

Translated from *Izvestiya Akademii Nauk. Seriya Khimicheskaya*, No. 5, pp. 897—903, May, 1998.

1066-5285/98/4705-0868 $20.00

Experimental

Methyl-substituted derivatives **2**—**6** were prepared by low-temperature cocondensation of atomic chromium and organic ligands using apparatus described previously.[11,12] The structures of the compounds were confirmed by the data of ^{1}H NMR spectroscopy and the results of chromatographic analysis of the products of acid decomposition. The complexes were purified by repeated sublimation *in vacuo*.

The vapor-phase absorption spectra were recorded on a Specord UV Vis (Carl Zeiss) spectrometer with the use of an evacuated heated quartz cell at 80—140 °C. The resolution was 30 cm^{-1}. Calibration was carried out using the spectrum of a benzene vapor. With the aim of revealing Rydberg bands, the vapor-phase spectrum of complex **6** was compared with the spectrum of a solution of this compound in *n*-heptane, which was recorded on the same instrument in an evacuated quartz cell at ~20 °C.

Results and Discussion

The refined frequencies of the Rydberg bands (Table 1) in the spectra of complexes **2**—**6**, the ionization limits, and the quantum defects agree well with the published data.[2—9] The accuracy of determination of peak maxima and, therefore, the accuracy of calculations of ionization potentials are limited by the intrinsic Rydberg band width, which increases in going from complex **1** to its methyl-substituted derivatives. This broadening can be caused by an increase in the interaction between Rydberg and valence-shell excited states as well as by the overlap of allowed vibronic components of Rydberg transitions the number of which increases as the symmetry is lowered. The assignments given in Table 1 were based on the analysis of the term values and the quantum defects as well as of the selection rules for optical transitions from the $3d_{z^2}$ orbital.

Depending on the mutual orientation of the ligands, molecule **1** may belong to the point symmetry group D_{6h}, D_{6d}, or D_6, molecules **2**—**4** may belong to the group C_{2v}, C_{2h}, or C_2, and molecule **5** may belong to the group D_{3h}, D_{3d}, or D_3. Correlations of irreducible representations,[13,14] according to which Rydberg states of

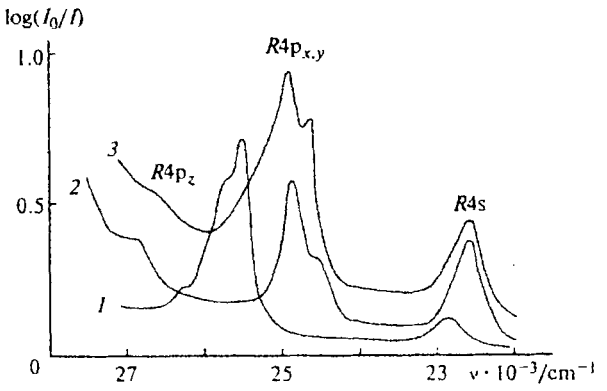

Fig. 1. Vapor-phase absorption spectra of complexes **2** (*1*), **3** (*2*), and **4** (*3*) in the region of the *R*4s and *R*4p transitions.

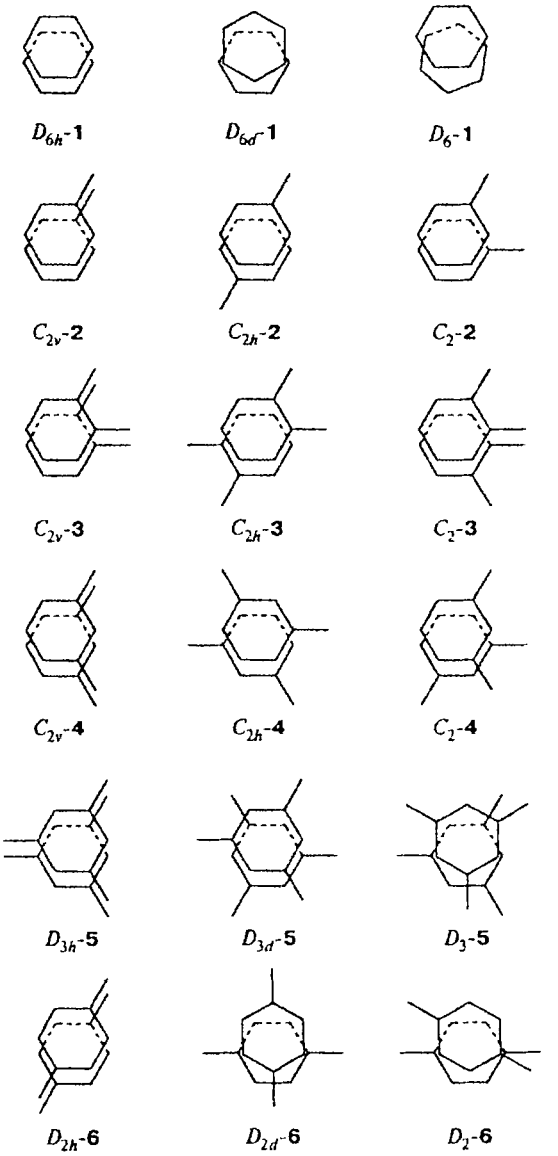

complex **1** are transformed as the symmetry is lowered, are given in Table 2. In going from compound **1** to derivatives **2**—**4**, the degenerate levels $Rnp(e_{1u})$ are split into two components. This splitting can be revealed based on the analysis of the structure of the *R*4p transitions.

The band of the $R4p_{x,y}$ transition in the spectrum of complex **2** (Fig. 1) consists of a peak with a maximum at 25530 cm^{-1} and shoulders located on the long-wavelength side at 25800, 26000, and 26400 cm^{-1}. The Gaussian analysis of the spectrum (Fig. 2) made it possible to reveal five peaks, whose parameters are given in Table 3.

The separations of the peaks at 25740 and 25990 cm^{-1}, which make a contribution to the shoulders at 25800 and 26000 cm^{-1}, from the Gaussian at 25520 cm^{-1} (see

Table 1. Frequencies (ν/cm^{-1}), term values (T/cm^{-1}), effective principal quantum numbers (n^*), and assignment of the Rydberg transitions in molecules **2**—**6**

$(\eta^6$-$C_6H_5Me)_2Cr$ [a]			$(\eta^6$-1,2-$Me_2C_6H_4)_2Cr$ [b]			$(\eta^6$-1,3-$Me_2C_6H_4)_2Cr$ [c]			$(\eta^6$-1,3,5-$Me_3C_6H_3)_2Cr$ [d]			$(\eta^6$-1,4-$Me_2C_6H_4)_2Cr$ [e]			Assignment
ν	T	n^*	ν	T	n^*	ν	T	n^*	ν	T	n^*	ν	T	n^*	
22870	19810	2.35	22570	18890	2.41	22500	18990	2.40	22400*f*	17960	2.47	22700*f*	18680	2.42	*R*4s
25530	17150	2.53	24480*f*	16980	2.54	24600	16890	2.55	25330*f*	15030	2.70	24670	16710	2.56	*R*4p$_{x,y}$
—	—	—	24780	16680	2.56	24870	16620	2.57	—	—	—	—	—	—	*R*4p$_{x,y}$
—	—	—	26900*f*	14560	2.75	26600*f*	14890	2.71	—	—	—	—	—	—	*R*4p$_z$
30000*f*	12680	2.94	29200*f*	12260	2.99	29100*f*	12390	2.98	28130	12230	2.98	—	—	—	*R*4d
32800*f*	9880	3.33	—	—	—	31900*f*	9590	3.38	—	—	—	—	—	—	*R*5s
34220	8460	3.60	32700	8760	3.54	32580*f*	8910	3.51	30800	9560	3.39	32570*f*	8810	3.53	*R*5p$_{x,y}$
—	—	—	—	—	—	32980	8510	3.59	—	—	—	—	—	—	*R*5p$_{x,y}$
34860*f*	7820	3.75	33530	7930	3.72	33870	7620	3.79	32590	7770	3.76	33520	7860	3.74	*R*5p$_z$
35920*f*	6760	4.03	34700*f*	6760	4.03	34750*f*	6740	4.04	33720*f*	6640	4.07	34770*f*	6610	4.07	*R*5d
36620*f*	6060	4.26	35180*f*	6280	4.18	35270*f*	6220	4.20	—	—	—	35210*f*	6170	4.22	*R*5d
37460	5220	4.59	—	—	—	36130*f*	5360	4.52	34800	5560	4.44	—	—	—	*R*6p$_{x,y}$
—	—	—	—	—	—	36280	5210	4.59	—	—	—	—	—	—	*R*6p$_{x,y}$
37800*f*	4880	4.74	36550	4910	4.73	36730	4760	4.80	35550*f*	4810	4.77	36480	4900	4.73	*R*6p$_z$
39180	3500	5.60	—	—	—	37930	3560	5.55	36600	3760	5.40	—	—	—	*R*7p$_{x,y}$
39480*f*	3200	5.86	38120	3340	5.73	38200*f*	3290	5.78	36930*f*	3430	5.66	38040	3340	5.73	*R*7p$_z$
40170	2510	6.61	—	—	—	38940	2550	6.56	37660	2700	6.38	—	—	—	*R*8p$_{x,y}$
—	—	—	39020	2440	6.71	39110*f*	2380	6.79	—	—	—	38970	2410	6.75	*R*8p$_z$
40800	1880	7.64	—	—	—	39590	1900	7.60	38400	1960	7.48	—	—	—	*R*9p$_{x,y}$
—	—	—	39620	1840	7.72	39670*f*	1820	7.76	—	—	—	39530	1850	7.70	*R*9p$_z$
—	—	—	—	—	—	40000	1490	8.58	38830	1530	8.47	—	—	—	*R*10p$_{x,y}$
—	—	—	—	—	—	—	—	—	—	—	—	39940	1440	8.73	*R*10p$_z$
—	—	—	—	—	—	40310	1180	9.64	39130	1230	9.45	—	—	—	*R*11p$_{x,y}$
—	—	—	—	—	—	40530	960	10.69	—	—	—	—	—	—	*R*12p$_{x,y}$

[a—e] The parameters of the most intense *Rnp* series:
[a] I = (5.292±0.007) eV, δ = 1.40;
[b] I = (5.141±0.007) eV, δ = 1.28;
[c] I = (5.144±0.005) eV, δ = 1.42;
[d] I = (5.004±0.007) eV, δ = 1.56;
[e] I = (5.131±0.005) eV, δ = 1.27.

f Shoulder.

Table 2. Correlation of the irreducible representations of the excited states of molecules **1**—**6**, which correspond to the transitions of the $3d_{z^2}$ electron to the Rydberg *ns*, *np*, and *nd* orbitals

Rydberg orbital	1			5			6			2—4		
	D_{6h}	D_{6d}	D_6	D_{3h}	D_{3d}	D_3	D_{2h}	D_{2d}	D_2	C_{2h} ($C_2 = y$)	C_{2v} ($C_2 = x$)	C_2 ($C_2 = x$)
Rns	$A_{1g}(f)$	$A_1(f)$	$A_1(f)$	$A_1'(f)$	$A_{1g}(f)$	$A_1(f)$	$A_g(f)$	$A_1(f)$	$A(f)$	$A_g(f)$	$A_1(x)$	$A(x)$
Rnp$_x$	$E_{1u}(x, y)$	$E_1(x, y)$	$E_1(x, y)$	$E'(x, y)$	$E_{1u}(x, y)$	$E(x, y)$	$B_{3u}(x)$	$E(x, y)$	$B_3(x)$	$B_u(x)$	$A_1(x)$	$A(x)$
Rnp$_y$	$E_{1u}(x, y)$	$E_1(x, y)$	$E_1(x, y)$	$E'(x, y)$	$E_{1u}(x, y)$	$E(x, y)$	$B_{2u}(y)$	$E(x, y)$	$B_2(y)$	$A_u(y)$	$B_2(y)$	$B(y, z)$
Rnp$_z$	$A_{2u}(z)$	$B_2(z)$	$A_2(z)$	$A_2''(z)$	$A_{2u}(z)$	$A_2(z)$	$B_{1u}(z)$	$B_2(z)$	$B_1(z)$	$B_u(z)$	$B_1(z)$	$B(y, z)$
Rnd$_{x^2-y^2}$	$E_{2g}(f)$	$E_2(f)$	$E_2(f)$	$E'(x, y)$	$E_g(f)$	$E(x, y)$	$A_g(f)$	$B_1(f)$	$A(f)$	$A_g(f)$	$A_1(x)$	$A(x)$
Rnd$_{xy}$	$E_{2g}(f)$	$E_2(f)$	$E_2(f)$	$E'(x, y)$	$E_g(f)$	$E(x, y)$	$B_{1g}(f)$	$B_2(z)$	$B_1(z)$	$B_g(f)$	$B_2(y)$	$B(y, z)$
Rnd$_{xz}$	$E_{1g}(f)$	$E_5(f)$	$E_1(x, y)$	$E''(f)$	$E_g(f)$	$E(x, y)$	$B_{2g}(f)$	$E(x, y)$	$B_2(y)$	$A_g(f)$	$B_1(z)$	$B(y, z)$
Rnd$_{yz}$	$E_{1g}(f)$	$E_5(f)$	$E_1(x, y)$	$E''(f)$	$E_g(f)$	$E(x, y)$	$B_{3g}(f)$	$E(x, y)$	$B_3(x)$	$B_g(f)$	$A_2(f)$	$A(x)$
Rnd$_{z^2}$	$A_{1g}(f)$	$A_1(f)$	$A_1(f)$	$A_1'(f)$	$A_{1g}(f)$	$A_1(f)$	$A_g(f)$	$A_1(f)$	$A(f)$	$A_g(f)$	$A_1(x)$	$A(x)$

Note. The polarizations of the allowed electric dipole transitions (*x*, *y*, *z*) are given in parentheses after the irreducible representations, and the symmetry-forbidden transitions (f) are denoted.

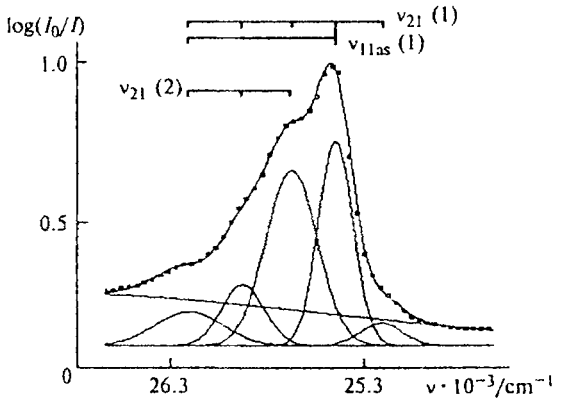

Fig. 2. Gaussian analysis of the $R4p_{x,y}$ band in the spectrum of complex **2**. The points correspond to the experimental spectral line.

Table 3. Positions of the maxima (ν), separations from the 0_0^0 transition (Δν), peak widths at the half-height ($\Delta_{1/2}$), relative integral intensities (A_{rel}), and interpretation of the Gaussian components of the $R4p_{x,y}$ band in the spectrum of complex **2**

ν	Δν	$\Delta_{1/2}$	A_{rel}	Assignment[a]
	cm^{-1}			
25290	−230	260	13	$[21]_1^0$ (1)[b]
25520	0	210	100	0_0^0 (1)
25740	220	310	127	$[21]_0^1$ (1) + 0_0^0 (2)
25990	470	260	37	$[21]_0^2$ (1) + $[21]_0^1$ (2)
26270	750	410	32	$[11as]_0^1$ (1) + $[21]_0^3$ (1) + + $[21]_0^2$ (2)

[a] Vibronic components are denoted as $[k]_{v''}^{v'}$, where *k* is the normal vibration according to the classification accepted for the molecule of bis(η^6-benzene)chromium[15,16], v'' and v' are the vibrational quantum numbers of the levels of the ground and excited electron states, respectively.

[b] The numbers in parentheses denote the assignments of the vibronic levels to two Rydberg states.

Table 3) allow one to consider these peaks as members of the progression on the symmetric metal—ligand stretching vibration ν_{21} in analogy to complex **1** [10] (to facilitate a comparative analysis of vibronic structures of the bands, we denote vibrations of methyl-substituted derivatives using the vibrational notation for the unsubstituted complex[15,16]). However, the peak at 25740 cm^{-1} is substantially broader than the peak at 25520 cm^{-1} (0_0^0 transition). As a result, its integral intensity has the maximum value (see Table 3). This is attributable to the fact that the second 0_0^0 component of the $R4p_{x,y}$ transition, which appears if degeneracy of the e_{1u} levels is removed, also contributes to the Gaussian at 25740 cm^{-1}. In this case, the peak at 25990 cm^{-1} corresponds to the $[21]_0^1$ and $[21]_0^2$ components of two different electron transitions. The assignment of the vibronic levels to each of the two electron-excited states is given in parentheses in the last column of Table 3.

The $[21]_0^3$ (1) and $[21]_0^2$ (2) transitions can contribute to the peak at 26270 cm^{-1}. However, its high relative intensity (see Table 3) indicates that in this case, as in the case of an analogous peak in the spectrum of complex **1**,[10] the vibronic component $[11as]_0^1$ plays a decisive role. This component corresponds to the excitation of a totally symmetric umbrella vibration of the CH group in the $R4p_{x,y}$ (1) state. The weak long-wavelength Gaussian at 25290 cm^{-1} (see Fig. 1) is the "hot" band $[21]_1^0$ (1).

Unlike the spectrum of complex **2** in which two 0_0^0 components of the $R4p_{x,y}$ transition can be revealed only based on the Gaussian analysis, the corresponding peaks in the spectra of derivatives **3** and **4** are rather pronounced (see Fig. 1), and their relative intensities exclude an alternative assignment to vibronic excitations. At the same time, the $R4p_{x,y}$ bands in the spectra of these complexes show no evidence of vibrational structure, which can be associated with the substantial overlap of the vibronic components of two electron

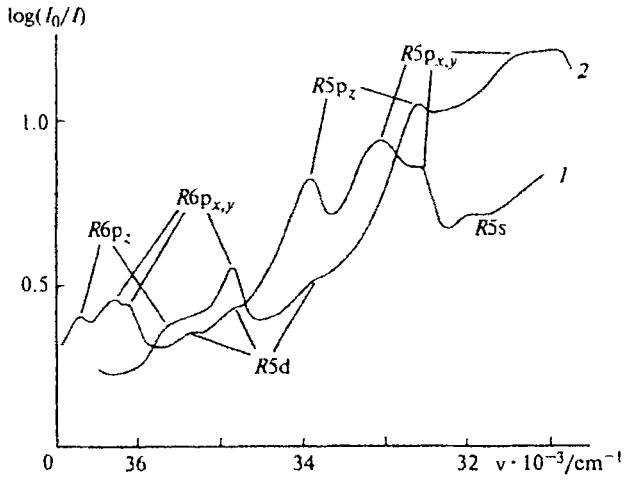

Fig. 3. Vapor-phase absorption spectra of complexes **4** (*1*) and **5** (*2*) in the region of the *R*5p and *R*6p transitions.

transitions. The splitting of the lower components of the long-wavelength *Rn*p series is most pronounced in the case of complex **4**. In the spectrum of **4**, two components can be also revealed for the $R5p_{x,y}$ and $R6p_{x,y}$ transitions (Fig. 3). The splitting for the $R5p_{x,y}$ excitation is even larger than for $R4p_{x,y}$ (see Table 1).

In the case of complex **5**, the $Rnp_{x,y}$ levels remain degenerate in each of the possible point symmetry groups (see Table 2). Therefore, the corresponding bands should not be split. It is difficult to judge the structures of the $R4p_{x,y}$ and $R5p_{x,y}$ transitions in the spectrum of compound **5** (in the former case, because of the low relative intensity, and in the latter case, because of the broadening caused by an admixture of the valence-shell excitation). The $R6p_{x,y}$ band narrows substantially in going from complex **4** to complex **5** (see Fig. 3), which is in agreement with the expected result.

In the spectra of compounds **3** and **4**,[5,8,9] the components of the Rnp_z series, many of which have pronounced maxima (see, for example, Fig. 3), are also clearly seen. In the case of complex **3**, the Rnp_z series at $n > 5$ is more intense than $Rnp_{x,y}$, which results in the difference in the quantum defects determined from the maxima of the short-wavelength Rydberg bands (see Table 1). The transition to the $R4p_z$ level, which is not observed in the spectra of compounds **1**, **2**, and **5**, appears as a shoulder at 26900 and 26600 cm^{-1} in the spectra of complexes **3** and **4**, respectively (see Fig. 1). Its assignment was based on the term values (see Table 1), which are close to the *T* value for the short-wavelength component of the *R*4p transition in the spectrum of $(\eta^6\text{-}C_6H_6)_2V$ (15650 cm^{-1})[9] and to the $T(R3p_z)$ value for free benzene (14780 cm^{-1}),[1] as well as on the n^* values (see Table 1), which confirm that the above-mentioned transition belongs to the Rnp_z series.

In some cases, the $3d_{z^2} \rightarrow Rns$ and $3d_{z^2} \rightarrow Rnd$ transitions become allowed (see Table 2) as a result of lowering of the symmetry owing to introduction of methyl groups. Actually, the bands which were assigned to the *Rn*s and *Rn*d excitations ($n = 4$ and 5) are observed in the spectra of complexes **2**—**4**.[5,8,9] In Fig. 1, the *R*4s bands in the spectra of compounds **2**—**4** are clearly seen. In the case of complex **5**, the $3d_{z^2} \rightarrow Rns$ transitions are forbidden, and only one *R*5d band is observed at 33720 cm^{-1} (see Fig. 3). The forbidden *R*4s transition may contribute[5,9] to the weak shoulder at 22400 cm^{-1}. The *Rn*s and *Rn*d term values of $(\eta^6\text{-arene})_2Cr$ (see Table 1) reported in this work for the first time agree well with the values obtained for mixed sandwich complexes,[17—23] which confirms the validity of the suggested assignment.

According to the selection rules, for molecules **2**—**4** the *Rn*s and *Rn*d transitions from the $3d_{z^2}$ orbital are allowed only in the case of the symmetry C_{2v} or C_2 (see Table 2). Therefore, the appearance of the intense *R*4s bands in the spectra indicates that in the gas phase these compounds adopt predominantly conformations that correspond to these point groups (but not to the group C_{2h}, although it is this geometry that corresponds to the minimum repulsion between the methyl groups). The symmetry group C_2 is more probable because in this case the mutual repulsion is smaller and a larger number of orientations of the rings is possible. In the case of complex **5**, the maximum distance between the substituents (and, therefore, the minimum repulsion) should occur in the conformation with the symmetry D_{3d}. However, the presence of the *R*5d band (whose intensity relative to the *R*5p and *R*6p peaks is comparable with the intensities of analogous bands in the spectra of complexes **3** [5,8,9] and **4**; see Fig. 3) in the spectrum of compound **5** is indicative of a substantial contribution of the conformations with the symmetry D_{3h} and/or D_3 in which the *Rn*d excitations are symmetry-allowed (see Table 2). Therefore, the analysis of the Rydberg structure provides information on the geometry of the molecules of bisarenechromium complexes in addition to the data on the mutual arrangement of the levels. In this connection, the spectrum of compound **6** is of particular interest.

Unlike complexes **3** and **4**, molecule **6** may belong to the point group D_{2h}, D_{2d}, or D_2. From the viewpoint of the molecular symmetry, this complex "fills the gap" between compound **5** and compounds **3** and **4** (see Table 2). In all the above-mentioned groups, the $3d_{z^2} \rightarrow Rns$ transitions are forbidden according to the selection rules, the *Rn*d excitations are allowed under the D_{2d} and D_2 symmetry, and the splitting of the $Rnp_{x,y}$ states may be observed in the case of the symmetry groups D_{2h} and D_2 (see Table 2).

The vapor-phase spectrum of complex **6** reveals the clearly defined Rydberg structure. This structure disappears in going to the condensed phase (Fig. 4). In the short-wavelength region of the spectrum, one Rydberg series with the quantum defect $\delta = 1.27$ can be observed. The value of this defect is very similar to the value of δ for the Rnp_z series in the spectrum of complex **3** (1.28) and differs only slightly from the quantum defect of the Rnp_z

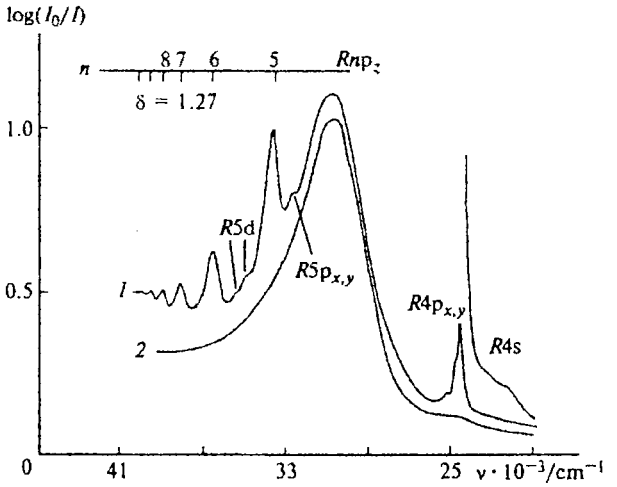

Fig. 4. Electronic absorption spectrum of complex **6** in the vapor phase (*1*) and in a solution in heptane (*2*).

series in the spectrum of compound **4** (1.21). Based on the value of δ, the series observed for complex **6** should be assigned to the $3d_{z^2} \rightarrow Rnp_z$ transitions. The value I = 41380±40 cm^{-1} (5.131±0.005 eV), which we determined for the first time, is slightly lower than the first ionization potentials of compounds **3** and **4**.

As in the case of compound **3**, the absence of the extended $Rnp_{x,y}$ series in the spectrum of complex **6** is attributable to low relative intensities of its members, which is clearly exemplified by the *R*5p transitions. The intense peak at 33520 cm^{-1} corresponds to the $3d_{z^2} \rightarrow R5p_z$ excitation, whereas only the relatively weak shoulder at 32570 cm^{-1} (see Table 1) may be assigned to the transition to the $R5p_{x,y}$ level based on the T and n^* values (see Fig. 4). The relative integral intensities of the lower Rydberg transitions, which were estimated based on the Gaussian analysis of the spectra of bisxylene chromium complexes and on the comparison of the peak areas, are given in Table 4. In all the cases, the $R5p_z$ peak area was taken to be 100. It is seen that the ratio of the intensities of the $R5p_{x,y}/R5p_z$ bands decreases rapidly in the series of compounds **4**, **3**, and **6**.

At the same time, the long-wavelength region of the spectrum of complex **6** shows an intense narrow peak at 24670 cm^{-1}, which, judging from the term value (see Table 1), may be associated only with the $3d_{z^2} \rightarrow R4p_{x,y}$ transition. Its relative intensity is similar to the corresponding values for complexes **3** and **4** (see Table 4). In contrast, the $R4p_z$ transition, which is observed in the spectra of complexes **3** and **4**, is absent in the spectrum of compound **6**. It should be noted that even for complexes **2** and **3**, the relative intensities of the $R4p_z$ bands differ from each other (see Table 4). Therefore, the difference in the arrangement of two methyl groups in the benzene rings of the three bisxylenechromium complexes is noticeably reflected (differently for n = 4 and n = 5) in the relative intensities of the lower Rnp transitions.

Table 4. Relative integral intensities of the lower Rydberg transitions in the spectra of complexes **3**, **4**, and **6**

Transition	A_{rel}			Transition	A_{rel}		
	3	**4**	**6**		**3**	**4**	**6**
*R*4s	14	14	—	*R*5s	—	15	—
$R4p_{x,y}$	20	32	29	$R5p_{x,y}$	43	147	15
$R4p_z$	12	1	—	$R5p_z$	100	100	100
*R*4d	27	19	—	*R*5d	30[a]	32[a]	23

[a] Total intensity of the observed components.

According to the selection rules (see Table 2), the spectrum of compound **6**, unlike the spectra of complexes **3** and **4**, does not reveal the intense *R*4s transition. This excitation is symmetry-forbidden and may contribute only to the weak shoulder at 22700 cm^{-1} (see Fig. 4). As in the case of complexes **3** and **4**, the spectrum of compound **6** has only two shoulders between the second and the third members of the Rnp series. Based on the T and n^* values (see Table 1), these shoulders should be assigned to the $3d_{z^2} \rightarrow R5d$ excitations. The relative intensities of the *R*5d transitions for the three bisxylene complexes have similar values (see Table 4). Based on this fact, it can be concluded that the conformations D_{2d} and D_2 are more probable for molecule **6** than the conformation D_{2h} in which the Rnd excitations are symmetry-forbidden.

In the point group D_{2d}, the $Rnp_{x,y}$ levels are doubly degenerate, whereas in the group D_2 this degeneracy is removed (see Table 2). If degeneracy is absent, the spectrum of complex **6** would be expected to have two separate 0_0^0 components of the $R4p_{x,y}$ transition, as in the case of complexes **3** and **4** (see Fig. 1). However, only one maximum is observed in the structure of the $R4p_{x,y}$ band in the spectrum of complex **6** (see Fig. 4). The Gaussian analysis of the spectrum (Fig. 5) made it possible to reveal only the members of the ν_{21} and ν_{11as} vibrational progressions. Unlike the toluene derivative,

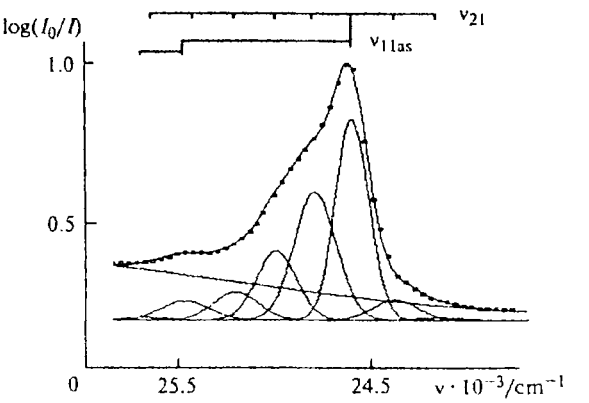

Fig. 5. Gaussian analysis of the $R4p_{x,y}$ band in the spectrum of complex **6**. The points correspond to the experimental spectral line.

Table 5. Parameters and assignment of the Gaussian components of the $R4p_{x,y}$ band in the spectrum of complex **6**

ν	Δν	$\Delta_{1/2}$	A_{rel}	Assignement
	cm^{-1}			
24220	–430	260	2	$[21]_2^0$
24440	–210	260	14	$[21]_1^0$
24650	0	190	100	0_0^0
24840	190	240	81	$[21]_0^1$
25030	380	230	41	$[21]_0^2$
25230	580	260	19	$[21]_0^3$
25490	840	280	14	$[11as]_0^1 + [21]_0^4$
25690	1040	260	2	$[11as]_0^1[21]_0^1 + [21]_0^5$

Note. The notations of the parameters of the Gaussians and the assignments are given in Table 3.

the distribution of the intensities in the ν_{21} progression (Table 5) has no anomalies, which could suggest the presence of the second 0_0^0 component. Therefore, the structure of the lower Rydberg p-transition in the spectrum of complex **6** indicates that the $R4p_x$ and $R4p_y$ states have equal or very similar energies. This, in turn, indicates that the angle between the projections of the lines that pass through the C atoms of the methyl groups of the ligands onto the plane that is parallel to the planes of the rings is equal to 90° (D_{2d}) or, at least, is close to the right angle (D_2). Therefore, in this case the study of the Rydberg structure provides information on the molecular geometry of sandwich compounds.

This work was financially supported by the Royal Chemical Society and the Russian Foundation for Basic Research (Project No. 96-15-97455).

References

1. M. B. Robin, *Higher Excited States of Polyatomic Molecules*, Academic Press, New York, 1985, **3**.
2. S. Yu. Ketkov, G. A. Domrachev, and G. A. Razuvaev, *Dokl. Akad. Nauk SSSR*, 1987, **292**, 890 [*Dokl. Chem.*, 1987 (Engl. Transl.)].
3. S. Yu. Ketkov, G. A. Domrachev, and G. A. Razuvaev, *Zh. Obshch. Khim.*, 1987, **57**, 967 [*J. Gen. Chem. USSR*, 1987, **57** (Engl. Transl.)].
4. S. Yu. Ketkov, G. A. Domrachev, and G. A. Razuvaev, *Optika i Spektroskopiya*, 1987, **62**, 227 [*Opt. Spectrosc. USSR*, 1987, **62** (Engl. Transl.)].
5. S. Yu. Ketkov, G. A. Domrachev, and G. A. Razuvaev, *Optika i Spektroskopiya*, **63**, 284 [*Opt. Spectrosc. USSR*, 1987, **63** (Engl. Transl.)].
6. S. Yu. Ketkov, G. A. Domrachev, and G. A. Razuvaev, *Zh. Fiz. Khim.*, 1987, **61**, 1682 [*J. Phys. Chem. USSR*, 1987, **61** (Engl. Transl.)].
7. G. A. Domrachev, S. Yu. Ketkov, and G. A. Razuvaev, *J. Organomet. Chem.*, 1987, **328**, 341.
8. S. Yu. Ketkov, G. A. Domrachev, and G. A. Razuvaev, *Metalloorg. Khim.*, 1988, **1**, 40 [*Organomet. Chem. USSR*, 1988, **1** (Engl. Transl.)].
9. S. Yu. Ketkov, G. A. Domrachev, and G. A. Razuvaev, *J. Mol. Struct.*, 1989, **195**, 175.
10. S. Yu. Ketkov, J. C. Green, and C. P. Mehnert, *J. Chem. Soc., Faraday Trans.*, 1997, **93**, 2461.
11. Yu. A. Shevelev, *Tez. dokl. IV Vsesoyuz. konf. po khimii nizkikh temperatur* [*Abstrs. of Papers, All-Union Conf. on Low-Temperature Chemistry*], Izd. Moscow Univ., Moscow, 1988, 210 (in Russian).
12. F. G. N. Cloke and M. L. H. Green, *J. Chem. Soc., Dalton Trans.*, 1981, 1938.
13. G. Herzberg, *Molecular Spectra and Molecular Structure, III. Electronic Spectra of Polyatomic Molecules*, Van Nostrand, New York, 1966.
14. R. L. Flurry, Jr., *Symmetry Groups. Theory and Chemical Applications*, Prentice-Hall, Englewood Cliffs, 1980.
15. L. Schafer, J. F. Southern, and S. J. Cyvin, *Spectrochim. Acta*, 1971, **27A**, 1083.
16. R. G. Snyder, *Spectrochim. Acta*, 1959, **15**, 807.
17. S. Yu. Ketkov, *J. Organomet. Chem.*, 1994, **465**, 225.
18. S. Yu. Ketkov, *Optika i Spektroskopiya*, 1992, **72**, 1088 [*Opt. Spectrosc. USSR*, 1992, **72** (Engl. Transl.)].
19. S. Yu. Ketkov, *J. Organomet. Chem.*, 1994, **465**, 225.
20. S. Yu. Ketkov, *Izv. Akad. Nauk, Ser. Khim.*, 1994, 634 [*Russ. Chem. Bull.*, 1994, **43**, 583 (Engl. Transl.)].
21. J. C. Green, M. L. H. Green, C. N. Field, D. K. P. Ng, and S. Yu. Ketkov, *J. Organomet. Chem.*, 1995, **501**, 107.
22. J. C. Green and S. Yu. Ketkov, *Organometallics*, 1996, **15**, 4747.
23. S. Yu. Ketkov and J. C. Green, *J. Chem. Soc., Faraday Trans.*, 1997, **93**, 2467.

Received December 15, 1997